Decomposition of NO on tungsten carbide and molybdenum carbide surfaces

Minghui Zhang [a], Henry H. Hwu [a], Mark T. Buelow [a], Jingguang G. Chen [a,*],
Todd H. Ballinger [b] and Paul J. Andersen [b]

[a] *Center for Catalytic Science and Technology, Department of Materials Science and Engineering, University of Delaware,*
Newark, DE 19716, USA
E-mail: jgchen@udel.edu
[b] *Johnson Matthey, Wayne, PA 19087, USA*

Received 9 April 2001; accepted 7 August 2001

The decomposition of ^{15}NO on C/W(111), C/W(110), and on monolayer and bulk C/Mo/W(111) surfaces is compared based on temperature-programmed desorption (TPD) and Auger electron spectroscopy (AES) measurements. Our results indicate that the decomposition of ^{15}NO occurs readily over all surfaces, and the only ^{15}N-containing reaction products are $^{15}N_2$ and $^{15}N_2O$ under our experimental conditions. Much higher surface reactivity for ^{15}NO decomposition was observed over the more open-structured C/W(111) surface, with a value of 0.68 ^{15}NO/W, in contrast to the surface reactivity of 0.24 ^{15}NO/W over the close-packed C/W(110) surface. The selectivity of these two ^{15}N-containing reaction products depends on the structure of the substrates as well. The more open-structured C/W(111) surface favors the production of $^{15}N_2$, with a product selectivity of $^{15}N_2$ being approximately 87%. In contrast, the selectivity to $^{15}N_2$ is only about 52% on C/W(110). In addition, we have investigated the decomposition of ^{15}NO on C/Mo surfaces that were epitaxially grown on W(111). The selectivity of $^{15}N_2$ on C/Mo/W(111) surfaces is $\sim$88%, which is very similar to that observed on C/W(111). Finally, the general similarity between the DeNOx chemistry on carbides and on Pt-group metals will also be discussed.

KEY WORDS: DeNOx; tungsten carbide; molybdenum carbide

1. Introduction

It is well known that Pt-group metals have been used in catalytic converters to effectively abate automobile emissions. For instance, the three-way catalysts (TWC) contain Rh, Pd, or Pt components [1]. Pt is primarily used for the oxidation of CO and un-combusted hydrocarbons; Rh is essentially responsible for the reduction of NO_x due to the high activity and selectivity for the reduction of NO to N_2 [2,3]. Current federal exhaust emissions standards, based on the 1990 Clean Air Act Amendments (CAAA), require a vehicle emission of NO_x being less than 0.6 g/mile with a durability of 100 000 miles. Starting from 2004, a more severe standard will be enforced which mandates that the emission of NO_x be further reduced to 0.2 g/mile [4]. Considering the limited natural abundance of Pt-group metals, it is imperative that these precious metals should be more effectively utilized in order to meet the more stringent regulations. This has in turn motivated a larger number of studies examining the reaction of NO_x on well-defined surfaces of Pt-group metals. The main objective of these studies was to achieve a better understanding of the interaction of NO with Pt-group metals, which should provide input for the more efficient utilization of Pt-group metals in the TWC catalysts.

The NO dissociation reaction has been reported to be very sensitive to the surface structure of Pt single crystals. For example, Campbell *et al.* reported that the dissociation of NO on a perfect Pt(111) surface is negligible [5]. Gorte *et al.* observed that the surface of Pt(100) exhibits much higher reactivity towards the decomposition of NO than the (110) or (111) planes [6,7]. N_2O formation is a negligible reaction pathway under the above studies on Pt single crystals. However, an exception was observed from K-promoted Pt(111) [8]. Moreover, N_2O formation over supported Pt–Rh, supported Rh, and single crystal Rh catalysts has been recognized as an important reaction pathway in the NO–CO reaction [9]. The surface structure-sensitive nature of NO dissociation has been shown on Rh as well. For instance, the following surface activity order in the NO dissociation has been reported: (111), (110) $<$ (100) $<$ (331) $<$ (533) $<$ (321) [10,11]. The general trend manifested by qualitative studies is the higher dissociation of NO on the more open-structured and stepped Rh surfaces [11]. In addition, the NO–CO reaction exhibits very strong structural sensitivity from a previous study on single crystal Rh surfaces at high ($1\ \text{Torr} < P < 100\ \text{Torr}$) pressures. The Rh(111) and Rh(110) surfaces show substantial selectivity difference regarding the formation of N_2 and N_2O. The more open-structured Rh(110) surface produces almost entirely N_2 and the selectivity of N_2O is as low as 8%, while the selectivity of N_2O on the more closely-packed Rh(111) surface is always higher than 40% [12].

The primary motivation of our current work is to search for less expensive and more abundant alternative catalysts to replace Pt-group metals. The carbides of groups IV–VI early

---

[*] To whom correspondence should be addressed.

1011-372X/01/1100-0029$19.50/0

transition metals often show catalytic activities that are similar to Pt-group metals [13–15]. In the past our group has investigated the reactivities of carbide-modified surfaces by chemical probe reactions that mainly involve the C–H bond transformation [15]. For example, in the dehydrogenation of cyclohexene to benzene, we found that the benzene yield on carbide-modified W [16] and Mo [17] is similar to that on Pt(111). The observation of Pt-like properties of early transition metal carbides was the driving force for us to examine the decomposition of ^{15}NO on C/W(111), C/W(110), and on monolayer and bulk C/Mo/W(111) surfaces.

In this paper we will attempt to determine whether the carbide surfaces are similar to Pt-group metal surfaces regarding the decomposition of NO. In addition, we would like to investigate how the structure of the W substrate affects the activity and selectivity of ^{15}NO decomposition on C/W(111) and C/W(110) surfaces. Furthermore, monolayer and bulk C/Mo surfaces, which are produced on a W(111) substrate, are also examined in this work to determine how the decomposition of NO is affected by the different parent metals in carbides.

2. Experimental

The experiments described in this paper were conducted in an ultrahigh-vacuum (UHV) chamber that is equipped with Auger electron spectroscopy (AES), temperature-programmed desorption (TPD), low-energy electron diffraction (LEED), and ion sputtering. The tungsten single crystal was mounted on a precision manipulator by spot-welding to two Ta wires. The surface can be cooled by contact with a liquid nitrogen reservoir and heated resistively through the Ta mounting wires.

Sample preparation first entails cleaning by several cycles of sputtering with 2 kV Ne$^+$ bombardment at 300 K followed by annealing in vacuum to 1200 K. Carbon that cannot be removed by sputtering was cleaned by exposing to oxygen at 1000 K followed by annealing at 1200 K. This process was continued until there are no detectable impurities by AES. The C/W(111) thin film was made by several cycles of exposing W(111) to 3 L ($1\ \mathrm{L} = 1 \times 10^{-6}$ Torr s) cyclohexene at about 120 K followed by annealing to 1200 K in vacuum. Cyclohexene decomposes to produce gas-phase hydrogen and atomic carbon on the surface. The surface prepared in this fashion has a C/W atomic ratio of approximately 0.55 and exhibits a $(\sqrt{3} \times \sqrt{3})$R30° LEED pattern. Cyclohexene was used as the chemical agent for making carbides mainly due to our prior knowledge and characterization of C/W(111) surfaces prepared in the similar fashion [16].

The C/W(110) surface was synthesized by a similar procedure. The clean W(110) surface was obtained by several cycles of sputtering with 2 keV Ne$^+$ bombardment at 300 K followed by annealing in vacuum to 1200 K. Oxygen treatment was also employed to remove carbon atoms that cannot be removed by sputtering. The cleanliness of the W(110) surface is confirmed by AES. The C/W(110) surface is prepared by several cycles of exposing a W(110) surface to 3 L cyclohexene at 120 K and followed by heating to 1200 K. C/W(110) made by this approach has a C/W atomic ratio $\sim$0.55, which exhibits a quasi-hexagon (two-fold rotational symmetry) LEED pattern of the W(110) substrate.

The C/Mo/W(111) surfaces were prepared by exposing Mo/W(111) to cycles of cyclohexene treatment, using the same approach as applied in preparing the C/W(111) surface. The Mo/W(111) surfaces were prepared *via* physical vapor deposition of Mo, by resistively heating a Mo ribbon of $\sim$0.025 mm in thickness, onto W(111) at 700 K. The W(111) substrate with a 1.3 ML Mo coverage is referred to as monolayer Mo/W(111). The surface with an atomic ratio of $\mathrm{Mo/W} > 7.0$ is referred to as bulk Mo/W(111). The Mo/W(111) surfaces retain the (1×1) hexagon LEED pattern of the W(111) substrate. The bulk C/Mo/W(111) surface shows a mixture of $(\sqrt{3} \times \sqrt{3})$R30° and hexagon LEED patterns.

The TPD experiments involved first exposing the carbide surfaces to 10 L of ^{15}NO at 100 K. The surface was then heated at a constant rate of 3 K/s and the desorption products were measured with a mass spectrometer. Several desorption products were measured by monitoring $m/q = 31$ (^{15}NO), 30 ($^{15}N_2$), 28 (CO), 46 ($^{15}N_2O$), 47 ($^{15}NO_2$), 18 (H_2O or $^{15}NH_3$), 32 (O_2), and 2 (H_2). The only species to desorb appreciably from all surfaces were ^{15}NO, $^{15}N_2$, CO, and $^{15}N_2O$.

3. Results and discussion

3.1. NO decomposition on C/W(111) and C/W(110)

TPD results recorded after exposing the C/W(111) to 10 L of ^{15}NO at 100 K are shown in figure 1. The decomposition of ^{15}NO is clearly demonstrated by the desorption of several reaction products, $^{15}N_2$, CO, and $^{15}N_2O$. The decomposition occurs at temperatures as low as $\sim$167 K, as evident by the desorption of the $^{15}N_2O$ product at this temperature. At higher temperatures, most of the oxygen atoms, from the decomposition of ^{15}NO, combine with the carbon atoms of C/W(111) to produce gas-phase CO at 912 K. The atomic ^{15}N also recombines and desorbs as $^{15}N_2$ at the same temperature. No other desorption products are observed, including $^{15}NH_3$, $^{15}NO_2$, or O_2.

The observation that N_2 and CO desorb at exactly the same temperature (at 912 K on C/W(111) and at 894 K on C/W(110) as shown below) suggests the presence of surface intermediates containing the CNO or NCO moiety. However, such intermediates are not detected in our vibrational studies using high-resolution electron energy loss spectroscopy (HREELS). For example, figure 2 shows a comparison of the HREEL spectra recorded after the adsorption of 10 L NO on C/W(111) at 90 K and after heating to different temperatures. At 90 K, the relatively sharp mode at 1792 cm^{-1} is the ν(NO) stretching mode of chemisorbed

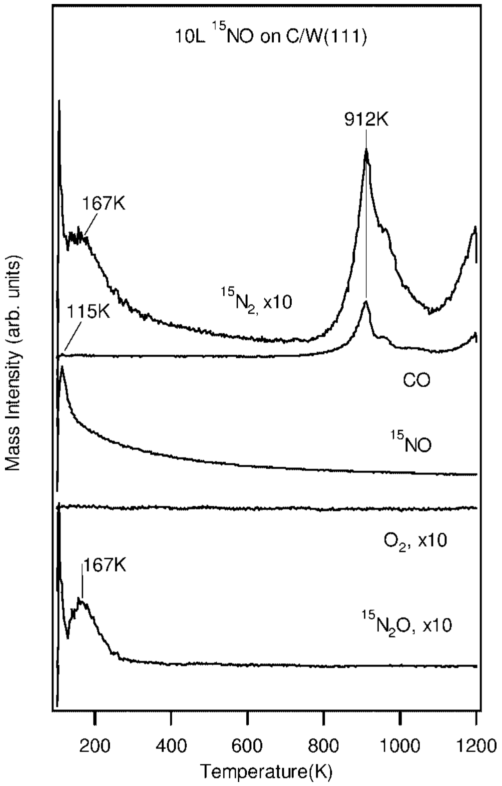

Figure 1. Temperature-programmed desorption spectra after exposing C/W(111) to 10 L ^{15}NO at 100 K and heating to 1200 K at a heating rate of 3 K/s.

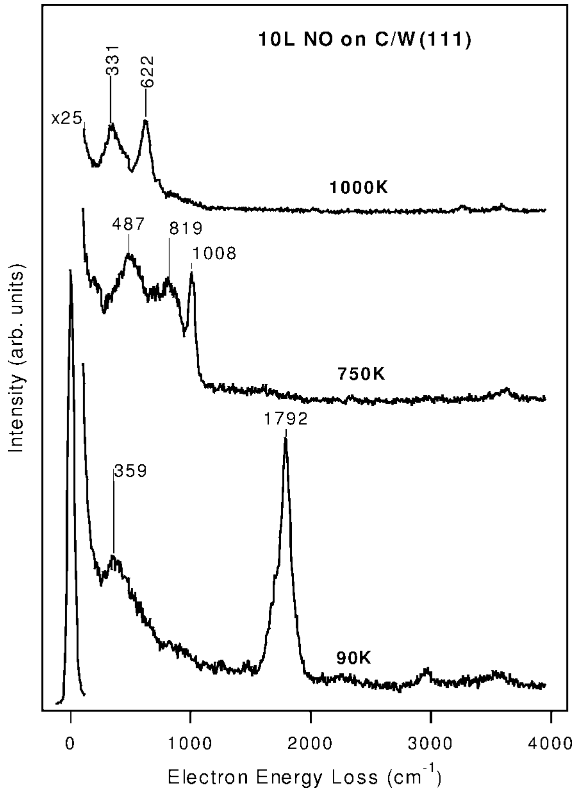

Figure 2. HREELS results following the decomposition of 10 L NO on C/W(111).

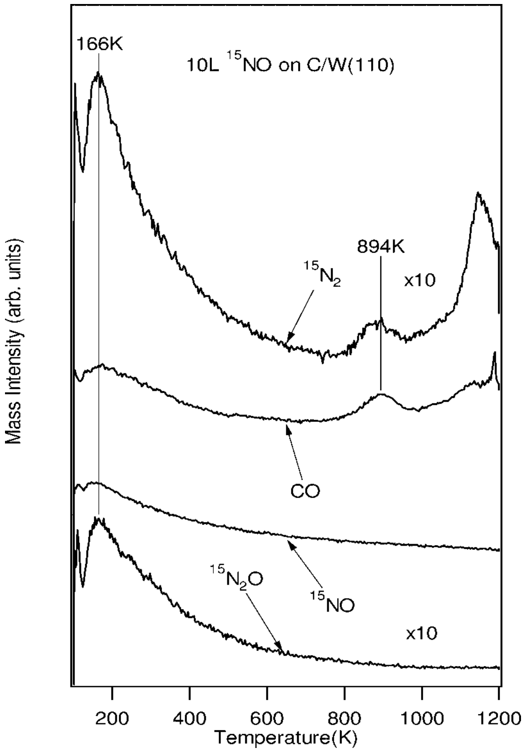

Figure 3. Temperature-programmed desorption spectra after exposing C/W(110) to 10 L ^{15}NO at 100 K and heating to 1200 K at a heating rate of 3 K/s.

NO; the broad bands at the low-frequency regions are related to the overlapping contribution from the ν(W–NO) and ν(W–C) modes. After heating the surface to 750 K, which is below the desorption temperature of N_2 and CO, NO molecules dissociate to produce atomic N and O, as indicated by the presence of the ν(W–N) mode at 819 cm^{-1} and the ν(W–O) mode at 1008 cm^{-1}. However, well-defined vibrational modes are not observed in the 750 K spectrum in the frequency region between 1200 and 2200 cm^{-1}, which should be expected if the CNO or NCO functional groups are present on the surface. More details about the HREELS studies of the decomposition mechanisms of NO on clean and chemically modified W(111) surfaces will be reported in a separate paper [18].

Because of the absence of the CNO or NCO intermediates, we cannot explain why the high-temperature desorption of N_2 and CO occurs at exactly the same temperature. We can only speculate that one of the recombinatory reactions ($N + N \rightarrow N_2$ or $C + O \rightarrow CO$) is an exothermal reaction, which might generate local heating that leads to the onset of the other recombinatory reaction. More studies are needed to determine the exact origin of the coincidental desorption of N_2 and CO.

The decomposition of ^{15}NO over the C/W(110) surface is investigated using TPD and is shown in figure 3. The TPD measurements were conducted after exposing the surface to 10 L ^{15}NO at 100 K. The C/W(110) surface is active towards the decomposition of ^{15}NO, as indicated by the detection of $^{15}N_2$, $^{15}N_2O$, and CO products. A relatively broad $^{15}N_2$

desorption peak is centered at approximately 166 K and another peak is observed at around 894 K. The low temperature $^{15}N_2$ peak is not contributed entirely by the cracking pattern of $^{15}N_2O$, which should give rise to a $^{15}N_2$ peak area that is approximately 11% that of $^{15}N_2O$ [19]. A very broad $^{15}N_2O$ desorption peak is detected in the temperature range between 140 and 600 K. The oxygen atoms that are produced by the decomposition of ^{15}NO remain on the surface and desorb only in the form of CO at 894 K. No molecular O_2 is detected in the TPD measurements.

By comparing the TPD results in figures 1 and 3, it is apparent that $^{15}N_2$ is preferentially produced on C/W(111) than on C/W(110). The selectivity of these two ^{15}N-containing products from C/W(111) can be estimated as follows: AES spectra were recorded after exposing C/W(111) to 10 L ^{15}NO at 100 K, and after the NO/C/W(111) surface was heated to 300 K. The latter temperature corresponds to the surface after the desorption of $^{15}N_2O$ from C/W(111). From the Auger measurements of $^{15}N/W$ and O/W atomic ratios, we estimated that the atomic ratio of N/O was to 1.0 at 100 K and 0.93 at 300 K. In addition, the atomic ratio of O/W is estimated to be approximately 0.68 at 300 K. Equations (1) and (2) describe the mass balance over the C/W(111) surface at 300 K:

$$a^{15}\mathrm{NO} \to \frac{a}{2}{}^{15}\mathrm{N_2O} + \frac{a}{2}\mathrm{O} \tag{1}$$

$$b^{15}\mathrm{NO} \to xb^{15}\mathrm{NO} + (1-x)b^{15}\mathrm{N} + (1-x)b\mathrm{O} \tag{2}$$

Symbol a represents the number of ^{15}NO molecules that are involved in the production of $^{15}N_2O$, and symbol b represents the number of ^{15}NO molecules remaining on the C/W(111), either in the molecular or decomposed form, after heating the surface to 300 K. Therefore, at 300 K we obtain the following relationships:

$$\mathrm{N/O} = \frac{b}{a/2+b} = 0.93, \tag{3}$$

$$\mathrm{O/W} = a/2 + b = 0.68. \tag{4}$$

a and b can be solved as 0.095 and 0.63 on the per W atom basis from equations (3) and (4), respectively. In order to compare the decomposition of NO on different surfaces, we define the surface reactivity as the total number of ^{15}NO molecules that undergo complete decomposition on the per W atom basis. The sum of $(a/2 + b)$ gives a surface reactivity of 0.68 $^{15}NO/W$ on C/W(111).

The selectivity of $^{15}N_2O$ from C/W(111) can be calculated from the values of a and b as follows, with symbol $S_{^{15}\mathrm{N_2O\_C/W(111)}}$ representing the $^{15}N_2O$ selectivity over C/W(111):

$$S_{^{15}\mathrm{N_2O\_C/W(111)}} = \frac{a}{a+b} = \frac{0.095}{0.095+0.63} = 13\%,$$
$$S_{^{15}\mathrm{N_2}} = 1 - S_{^{15}\mathrm{N_2O}} = 87\%.$$

Similarly, the mass balance on the C/W(110) surface can be described by equations (5) and (6),

$$c^{15}\mathrm{NO} \to \frac{c}{2}{}^{15}\mathrm{N_2O} + \frac{c}{2}\mathrm{O} \tag{5}$$

$$d^{15}\mathrm{NO} \to xd^{15}\mathrm{NO} + (1-x)d^{15}\mathrm{N} + (1-x)d\mathrm{O} \tag{6}$$

Symbol c represents the number of ^{15}NO molecules decomposing to produce $^{15}N_2O$ at 100–600 K, and symbol d represents the number of ^{15}NO molecules remaining on the C/W(110) surface, either in the molecular or decomposed form, after it was heated to higher temperatures. AES spectra were recorded after exposing C/W(110) to 10 L ^{15}NO at 120 K and flashed to 600 K. The O/W atomic ratio on C/W(110) was estimated as 0.24 after the surface heated to 600 K. This leads to the following relationship:

$$\mathrm{O/W} = \frac{c}{2} + d = 0.24. \tag{7}$$

The O/W atomic ratio gives rise to the surface reactivity of NO decomposition over C/W(110) as 0.24 $^{15}NO/W$, which corresponds to the total number of ^{15}NO undergoing complete decomposition on the per W atom basis.

The overall TPD peak area of $^{15}N_2$ from C/W(110) is the sum of the low-temperature (166 K) and high-temperature (894 K) peaks. The sum was then subtracted by 11% of the $^{15}N_2O$ peak area to remove the contribution from the cracking pattern of $^{15}N_2O$ to the low-temperature $^{15}N_2$ peak [19]. By comparing the relative TPD peak areas of $^{15}N_2O$ and $^{15}N_2$ from both C/W(110) and C/W(111), which are summarized in table 1, the relationship of c and d can be derived as the following:

$$\frac{c}{d} = \frac{1/1a}{0.98/6.11b} = 0.94. \tag{8}$$

By combining equations (7) and (8), the values of c and d can be estimated on the per W atom basis as follows:

$$c = 0.15,$$
$$d = 0.16.$$

Therefore, the selectivity of $^{15}N_2$ and $^{15}N_2O$ over C/W(110) can be estimated as follows:

$$S_{^{15}\mathrm{N_2\_C/W(110)}} = \frac{d}{c+d} = \frac{0.16}{0.16+0.15} = 52\%,$$
$$S_{^{15}\mathrm{N_2O\_C/W(110)}} = 1 - 52\% = 48\%.$$

From the above selectivity calculation, it is clear that the decomposition of ^{15}NO over C/W(111) and C/W(110) leads to a very different selectivity of ^{15}N-containing products. The more open-structured C/W(111) surface favors to produce the $^{15}N_2$ product, while the close-packed structure of C/W(110) produces nearly equal number of $^{15}N_2$ and $^{15}N_2O$. This observation clearly indicates the structure sensitivity in the decomposition of ^{15}NO.

3.2. NO decomposition over monolayer and bulk C/Mo/W(111)

The decomposition of ^{15}NO over monolayer C/Mo/W(111) and bulk C/Mo/W(111) surfaces is studied by TPD and is shown in figure 4. The TPD measurements were conducted after exposing the carbide surfaces to 10 L ^{15}NO at

Table 1
Surface reactivity and product selectivity.

Surface	Relative peak area[a]		*a*	*b*	*c*	*d*	Surface reactivity	$^{15}N_2$ selectivity
	$^{15}N_2O$	$^{15}N_2$					(#^{15}NO/W)	(%)
C/W(111)	1	6.11	0.095	0.63			0.68	87
C/W(110)	1	0.98			0.15	0.16	0.24	52
Monolayer C/Mo/W(111)	1	7.57	–	–	–	–	–	89
Bulk C/Mo/W(111)	1	6.98	–	–	–	–	–	88

[a] For ease of comparison the relative peak areas of $^{15}N_2O$ are normalized to a value of 1 on all surfaces.

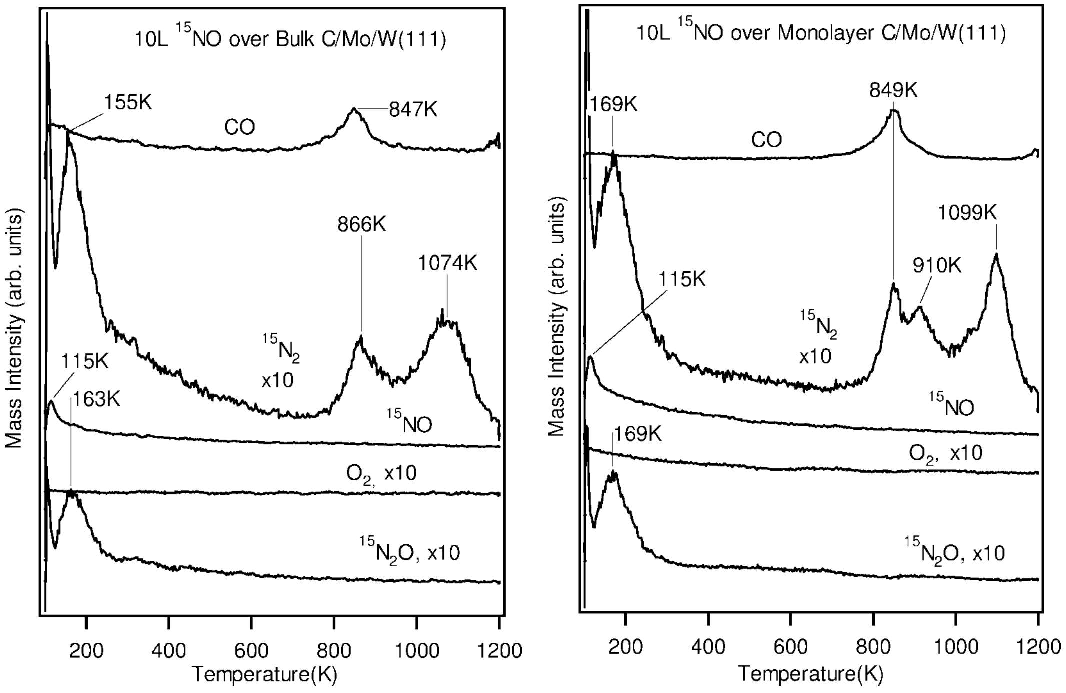

(a) (b)

Figure 4. Temperature-programmed desorption spectra after exposing bulk C/Mo/W(111) (a) and monolayer C/Mo/W(111) (b) to10 L ^{15}NO at 100 K and heating to 1200 K at a heating rate of 3 K/s.

100 K and heating to 1200 K. The two C/Mo/W(111) surfaces show nearly identical behavior in the decomposition of ^{15}NO. Both surfaces are very active towards the decomposition of ^{15}NO, and $^{15}N_2$ and $^{15}N_2O$ are the only ^{15}N-containing reaction products. The O atoms produced by the decomposition of ^{15}NO remain on the surface and desorb only in the form of CO at ~847 or ~849 K. No molecular O_2 is detected by mass spectrometry. Several relatively intense $^{15}N_2$ desorption peaks are observed at the indicated temperatures in figure 4. Three intense $^{15}N_2$ desorption peaks, shown in figure 4(a) at 155, 866, and 1074 K, are assigned the recombinative desorption of ^{15}N on the bulk C/Mo surface. Similarly, the N_2 desorption peaks on the monolayer C/Mo/W(111) surface (figure 4(b)) at 169, 849, and 1099 K, can also be assigned to the recombinative desorption of ^{15}N from carbide-modified Mo. The additional feature at 910 K is likely from the contribution from the C/W(111) substrate, suggesting that the W(111) surface is not completely covered by Mo at this coverage.

The selectivity of $^{15}N_2$ and $^{15}N_2O$ over the monolayer and bulk C/Mo/W(111) surfaces can be estimated by comparing their peak areas with those from C/W(111), as summarized in table 1. Nearly identical $^{15}N_2$ selectivity is found over the two C/Mo/W(111) surfaces with a value of ~88%. Consequently, the selectivity of $^{15}N_2O$ is ~12% over the two surfaces. Coincidently, the selectivity of ^{15}N-containing products on C/Mo/W(111) is nearly the same as that of C/W(111). This observation suggests that the product selectivity of ^{15}NO appears to be more sensitive to the structure of the substrate than to the identity of the parent metals.

3.3. Comparison with Pt-group metal surfaces

The structure-sensitive nature of NO dissociation has been observed in previous studies of the decomposition and reduction of NO over Pt-group metal surfaces. It is important to point out that W has the body-centered cubic (bcc) structure, and the W(110) plane corresponds to the most closely-packed surface. On the other hand, Pt and Rh have the face-centered cubic (fcc) structure, and the (111) plane is the most close-packed surface. As mentioned in section 1, one of the general trends in the decomposition of NO over Pt and Rh single crystal is that the more open-structured surfaces show higher surface reactivity in the dissociation of NO. For instance, a relatively high reactivity is observed in the decomposition of NO over Pt(100), in contrast to the negligible dissociation over the (111) plane [6,7]. Moreover, previous studies on Pt-group metal surfaces also reveal the structure-sensitivity in the product selectivity in the NO–CO reaction. For instance, the more open-structured Rh(110) surface produces almost entirely $^{15}N_2$ (92%), while on Rh(111) the $^{15}N_2O$ selectivity is higher than 40% [12].

Our results indicate that the decomposition of ^{15}NO occurs readily over all the carbide surfaces investigated in this work, and the only ^{15}N-containing reaction products are $^{15}N_2$ and $^{15}N_2O$ over all the surfaces. The structure-sensitive nature of NO decomposition is indicated by the different surface reactivity. For example, the total number of ^{15}NO undergoing dissociation is 0.68 $^{15}NO/W$ over the open-structured C/W(111) surface, in contrast to 0.24 $^{15}NO/W$ over closely-packed C/W(110) surface. Moreover, the product selectivity of $^{15}N_2$ and $^{15}N_2O$ is also very different between C/W(111) and C/W(110). The selectivity of $^{15}N_2$ over the more open-structured C/W(111) surface is about 87%. In contrast, the selectivity of $^{15}N_2$ over the more closely-packed C/W(110) is only about 52%. Comparing to the results on Pt-group metal surfaces mentioned above, there appears to be a general trend that more open-structured carbide and Pt-group metal surfaces show both higher surface reactivity and more desirable product selectivity (N_2) in the decomposition of NO.

4. Conclusions

The decomposition of ^{15}NO occurs readily over all carbide surfaces in this work, and ^{15}N-containing reaction products are $^{15}N_2$ and $^{15}N_2O$ only. These results demonstrate that the carbides of tungsten and molybdenum show similar or higher activities than Pt-group metals regarding the decomposition of NO. Moreover, both the selectivity of ^{15}N-containing products and surface reactivity in the decomposition of NO depend strongly on the structure of the substrates. The more open-structured C/W(111) exhibits higher surface reactivity in the decomposition of NO and favors to produce significantly more $^{15}N_2$ compared with the C/W(110) surface. The latter observation indicates that the reaction pathways of ^{15}NO are structure-sensitive, confirming previous studies of the decomposition of NO on Pt-group metal surfaces.

Acknowledgement

The authors would like to acknowledge Johnson Matthey and Delaware Research Partnership for financial support of this work. We also acknowledge partial support from Department of Energy, Basic Energy Sciences (Grant No. DE-FG02-00ER15104). We also like to thank H.-Y. Chen and P. Shady of Johnson Matthey for helpful discussion.

References

[1] E.S.J. Lox and B.H. Engler, in: *Handbook of Heterogeneous Catalysis*, eds. G. Ertl, H. Knözinger and J. Weitkamp (Wiley/VCH, New York/Weinheim, 1997) p. 1559.
[2] L.L. Hegedus, J.C. Summers, J.C. Schlatter and K. Baron, J. Catal. 56 (1979) 321.
[3] M. Shelef and G.W. Graham, Catal. Rev. Sci. Eng. 36 (1994) 433.
[4] G.C. Koltssakis and A.M. Stamatelos, Prog. Energy Combust. Sci. 23 (1997) 1.
[5] C.T. Campbell, G. Ertl and J. Segner, Surf. Sci. 115 (1982) 309.
[6] R.J. Gorte, L.D. Schmidt and J.L. Gland, Surf. Sci. 109 (1981) 367.
[7] R.J. Gorte and L.D. Schmidt, Surf. Sci. 111 (1981) 260.
[8] H. Wang, R.G. Tobin, C.L. Dimaggio, G.B. Fisher and D.K. Lamber, J. Chem. Phys. 107 (1997) 9569, and references therein.
[9] K.Y.S. Ng, D.N. Belton, S.J. Schmieg and G.B. Fisher, J. Catal. 146 (1994) 394, and references therein.
[10] H.A.C.M. Hendricks and B.E. Nieuwenhuys, Surf. Sci. 175 (1986) 185.
[11] G. Comelli, V.R. Dhanak, M. Kiskinova, K.C. Prince and R. Rosei, Surf. Sci. Rep. 32 (1998) 165.
[12] C.H.F. Peden, D.N. Belton and S.J. Schmieg, J. Catal. 155 (1995) 204, and references therein.
[13] S.T. Oysma and G.L. Haller, in: *Catalysis*, Spec. Rep., eds. G.C. Bond and G. Webb (The Chem. Soc., London, 1981) pp. 5, 333.
[14] S.T. Oysma, *The Chemistry of Transition Metal Carbides and Nitrides* (Blackie Academic and Professional, Glasgow, 1996).
[15] J.G. Chen, Chem. Rev. 96 (1996) 1477, and references therein.
[16] N. Liu, S.A. Rykov, H.H. Hwu, M.T. Buelow and J.G. Chen, J. Phys. Chem. B 105 (2001) 3894.
[17] J.G. Chen and B. Fruhberger, Surf. Sci. 367 (1996) L102.
[18] M.H. Zhang, H.H. Hwu, M.T. Buelow, J.G. Chen, T.B. Ballinger and P.J. Andersen, J. Catal., submitted.
[19] WWW. webbook.nist.gov.